ELECTRICAL DISCHARGE IN HONEYCOMB MONOLITH

KAROL HENSEL*, SATOSHI SATO, and AKIRA MIZUNO

Department of Astronomy, Earth Physics and Meteorology, Comenius University, Bratislava, 842-48 Slovakia, Department of Ecological Engineering, Toyohashi University of Technology, Toyohashi 441-8580, Japan
hensel@fmph.uniba.sk

Keywords: microplasmas, sliding discharge, honeycomb catalyst, flue gas treatment, emission spectroscopy

1. Introduction

Tree-way catalysts of honeycomb structure are used in gasoline automobiles for the exhaust gas cleaning. The performance of the catalysts strongly depends on the composition and the temperature of the exhaust gas. The catalysts can be ineffective, if the temperature of the exhaust gases is low or in case of an access of oxygen. One of the possibilities, how to improve the performance is to combine the catalyst with a non-thermal plasma. It is well-known that the combination of such plasma and catalyst in a hybrid system usually results in an improvement of gas treatment efficiency, carbon balance and reduction of suspended particles in the gas. In the past, there have been several attempts to generate the discharges inside the ceramics honeycomb monoliths[1,2]. Various cuts and slices of honeycomb monolith integrated with a system of electrodes of assorted geometries were applied to generate the plasma inside the channels of these catalysts. Despite the promising results obtained for NOx and VOC treatment several serious problems has been reported. One of them is a stability of the discharge and plasma generated inside thin and long channels of honeycomb monolith. The stability can be very much affected by the walls confining the discharge. Due to the loss of the charged particles on the walls of the capillaries, the onset and operating voltages is higher compared to non-confined system. A stable streamer discharge is very difficult to obtain, instead of that rather unstable sparking occur. When operating the discharge for a certain period of time in sparking mode, the mechanical breakdown of the ceramic walls and ultimate failure of the catalyst may occur. Therefore the generation of homogenous and stable plasma inside thin channels of honeycomb catalysts was found so far rather difficult.

In this paper we present a new method for the generation of the stable discharge plasma inside the honeycomb monolith. The idea behind this method is that instead of generating the discharge directly inside the channel, the discharge is generated outside the channels and subsequently extended into the channels. It is done by the generation of auxiliary discharge at one of the ends of the honeycomb monolith and application of the additional electric field across the monolith. This method is in fact a utilization of a technique used in the past for a sliding discharge generation[3,4]. The sliding discharge is a discharge generated on flat dielectrics by e.g. combination of AC and DC powers in three-electrode geometry. It is particularly important in aeronautics for active wing flow control by the electric wind produced by the discharge. We used the concept of the sliding discharge to generate the discharge inside the honeycomb monolith along the dielectric walls of the thin channel. The paper present basic characteristics of the sliding discharge inside the capillary channels, addressing the effects of the diameter, length of the channels and the applied voltage.

2. Experimental System

The simplified scheme of the experimental reactor equipped with relevant measuring systems is depicted on Fig. 1.

The reactor consisted of a cylindrical quartz tube of 26 mm diameter. The tube was filled with a bundle of quartz capillaries of 1–3 mm diameter and lengths of 2 or 3 cm. The capillaries were placed on the top of γ-Al_2O_3 pellet bed located at the bottom part of the tube. The bundle of transparent capillaries was used instead of ceramic honeycomb monolith in order to visually observe the discharges inside and to be able to apply the optical emission spectroscopy. The set of three electrodes consisted of a rod plugged in the middle of the pellet bed, aluminum foil wrapped around the quartz tube and a mesh electrode placed on the top of the capillaries. The rod was powered by AC high voltage of 50 Hz, the mesh by negative DC high voltage, and the foil was grounded. Negative DC was chosen to ensure discharge operation up to higher voltages without sparking. The amplitude and waveform of the applied voltages was measured by high voltage probes Tektronix P644A connected to the digital oscilloscope Tektronix TDS2014. The pellet bed discharge power was evaluated from Lissajous figures and the power of the discharge in capillaries as a product of DC voltage and a mean current. Optical measurements were performed by an emission spectrometer Ocean Optics SD2000 and the images were recorded by a digital camera Nikon D40x.

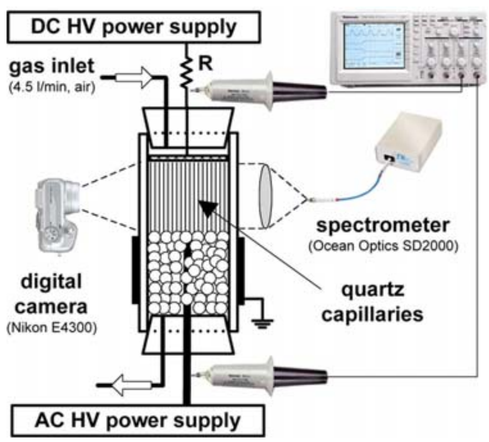

Fig. 1. **Experimental setup depicting discharge reactor and electric and optical measuring systems**

3. Results and Discussion

When AC voltage was applied on the rod electrode, the barrier discharge inside the pellet bed was formed. The discharge current waveform of the barrier discharge was typical by the current pulses of amplitudes of several tens of milliamps, which were superposed on the capacitive current bias component. The barrier discharge produced the plasma which served as a kind of ionizer. It produced charged particles and ionic space charges at the bottom of the bundle of glass capillaries. Upon the application of DC voltage on the mesh electrode the charges were accelerated through the capillaries toward the mesh electrode finally forming a sliding discharge. As a result, stable and homogenous plasma formation was observed inside the capillary channels.

Fig. 2 shows the typical voltage and current waveforms of the sliding discharge when negative DC was used. Compared to waveform of the barrier discharge, additional negative pulses can be recognized during the positive maximum of the applied voltage. They are the result of the sliding discharge propagation inside the capillaries. The discharge occurred only when the polarity of the rod and mesh electrode were opposite as result of the high potential difference across the capillaries. When the rod and the mesh were of the same polarity no sliding discharge was observed.

Fig. 3 present the images of the discharges taken by the digital camera for various amplitudes of the applied voltage. The images show the sliding discharge inside glass capillaries formed only when both AC and DC were applied. With AC only barrier discharge inside the pellet bed was formed, while with DC only a corona discharge at the mesh could be observed. The images also show the distribution of the discharge and the emission inside the capillaries was relatively homogenous. The stable sliding discharge operation was possible within a wide interval of both DC and AC applied voltages. The transition of the sliding discharge into a spark discharge was observed when too high applied voltages were used. The DC sparking voltage decreased with increasing the AC applied voltage and vice versa.

Excessive sparking was also observed when dry gas

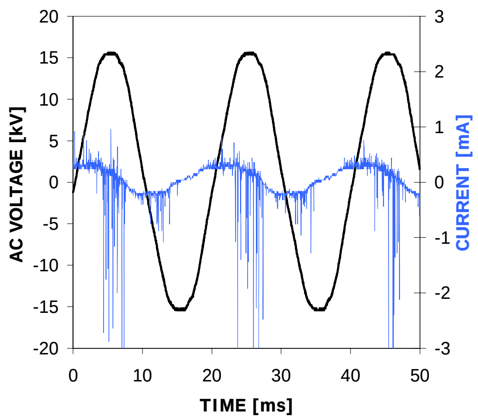

Fig. 2. **Waveforms of the applied voltage and discharge current of sliding discharge** [U_{AC} = 15 kV, U_{AC} = –16 kV]

Fig. 3. **Images of the discharge in capillaries** [diameter 2 mm, length 3 mm] **at different AC and DC applied voltages in ambient air:** (top left) the reactor, (top right) barrier discharge [U_{AC} = 16 kV, U_{DC} = 0 kV], (bottom left) corona discharge [U_{AC} = 0 kV, U_{DC} = –20 kV], (bottom right) sliding discharge [U_{AC} = 15 kV, U_{DC} = –16 kV]

mixtures were used. Fig. 4 shows the images of the discharge in dry nitrogen and ambient air, showing higher operational AC and DC applied voltages could be reached without sparking if moisture was present in the system. The origin of the effect is not fully understood, but it is assumed to be connected with the formation of water clusters which stabilize the discharge. The transition of the sliding discharge into a spark could also be suppressed by ballasting the DC line with the appropriate resistor, thus limiting the amplitude of the discharge current

Fig. 5 shows the power of the sliding discharge as a function of the DC applied voltage for various lengths of the capillaries and the AC voltages. The discharge power increased with both DC and AC applied voltages. The effect of AC voltage was however negligible since the power of the pellet bed discharge was one order of magnitude less than that of the sliding discharge. With extending the length of capillaries at a given DC voltage, the discharge current and power decreased. In contrast, a diameter of the capillary had marginal effect on the discharge power.

Emission spectroscopy is a method that provides valuable information on excited atomic and molecular states, enables the determination of the temperatures of the plasma and thus the level of non-equilibrium, and the gas temperature. Fig. 6 shows the emission intensity of the sliding discharge

Fig. 4. **Images of the discharge in capillaries** [diameter 2 mm, length 2 mm] **at different AC and DC applied voltages in:** (left) ambient air [U_{AC} = 15 kV, U_{DC} = −16 kV], (right) dry nitrogen [U_{AC} = 15 kV, U_{DC} = −10 kV]

based on the 0-0 spectral band (337 nm) of 2nd positive system of N_2 ($C_3\Pi_u$–$B_3\Pi_g$) as a function of the DC voltage. The intensity increased with both DC and AC applied voltages. In contrast to the negligible effect of AC voltage on the discharge power, its effect on the discharge emission was significant. The intensity also reflects a concentration of active species generated by the discharge. To minimize the power consumption but keep the same intensity, it seems appropriate to maximize AC and minimize DC applied voltage. The figure also shows the intensity decreased for longer capillaries as a result of decreasing discharge current.

Fig. 7 shows the emission intensity of the sliding discharge depending on the DC applied voltage for various diameters of capillaries. On contrary to the effect of the length of capillaries, the effect of the diameter was found negligible, especially at low DC applied voltage.

By using Specair software from N_2 ($C_3\Pi_u$–$B_3\Pi_g$) spectral bands we determined rotational and vibrational temperatures found the typical values 300 ± 30 K and 1800 ± 300 K, respectively. Rotational temperature was found independent of the applied voltages. The plasma generated by the sliding discharge is cold with a high level of non-equilibrium.

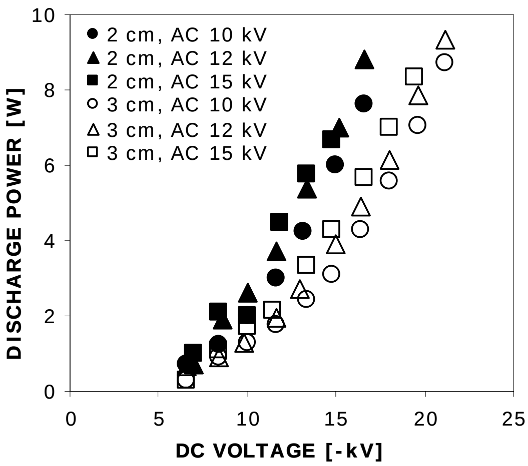

Fig. 5. **Discharge power as functions of negative DC applied voltage for various AC applied voltage and the length of capillaries** [diameter 2 mm, ambient air]

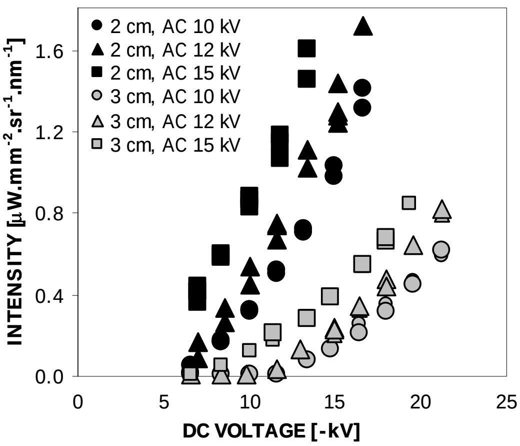

Fig. 6. **Discharge emission intensity as functions of negative DC applied voltage for various AC voltage and the length of capillaries** [diameter 2 mm, ambient air]

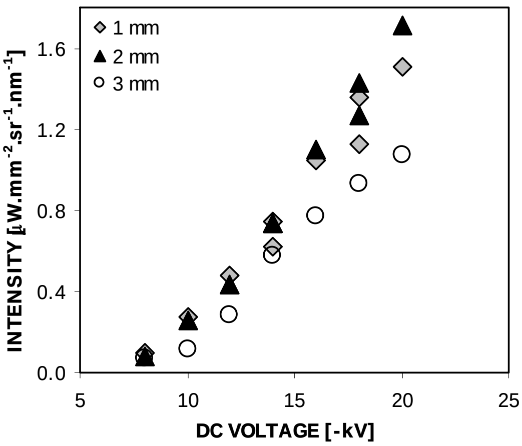

Fig. 7. **Emission intensity as functions of negative DC applied voltage for various diameters of capillaries** [length 20 mm, AC 10 kV]

4. Conclusions

Generation of microplasmas inside spatially confined geometry of bundle of glass capillaries (simulating honeycomb monolith structure) by using sliding discharge was presented. The paper introduced the fundamental physical properties of the discharge based on electrical and optical measurements. Sliding discharge inside honeycomb was generated by a superposition of AC barrier discharge in series with DC powered honeycomb monolith. The homogeneity and the stability of the discharge can be controlled by amplitude and polarity of the applied voltage and contents of moisture. The discharge generates relatively cold plasma with a high level of non-equilibrium.

Work was supported by Slovak Research and Development Agency grants APVT 20-032404, SK-FR-00506 and by Slovak Grant Agency grant 1/3041/06.

REFERENCES

1. Kim H. H.: *PhD Thesis*, Toyohashi University of Technology, Toyohashi (2000).
2. Blin-Simiand N., Tardiveau P., Risacher A., Jorand F., Pasquiers S.: Plasma Proc. Polym. *2*, 256 (2005).
3. Moreau E., Louste C., Touchard G.: J. Electrostat. *66*, 107 (2008).
4. Sosa R., Kelly H., Grondona D.: J. Phys. D: Appl. Phys. *41*, 035202 (2008).